Molecular Plant • Volume 6 • Number 2 • Pages 444–455 • March 2013 RESEARCH ARTICLE

Aequorin-Based Luminescence Imaging Reveals Stimulus- and Tissue-Specific Ca^{2+} Dynamics in *Arabidopsis* Plants

Xiaohong Zhu[a,1], Ying Feng[a], Gaimei Liang[a], Na Liu[a] and **Jian-Kang Zhu[a,b,1]**

a Department of Horticulture and Landscape Architecture, Purdue University, West Lafayette, IN 47907, USA
b Shanghai Center for Plant Stress Biology and Shanghai Institute of Plant Physiology and Ecology, Shanghai Institutes of Biological Sciences, Chinese Academy of Sciences, Shanghai 200032, China

ABSTRACT Calcium ion is a versatile second messenger for diverse cell signaling in response to developmental and environmental cues. The specificity of Ca^{2+}-mediated signaling is defined by stimulus-elicited Ca^{2+} signature and downstream decoding processes. Here, an Aequorin-based luminescence recording system was developed for monitoring Ca^{2+} in response to various stimuli in *Arabidopsis*. With the simple, highly sensitive, and robust Ca^{2+} recording, this system revealed stimulus- and tissue-specific Ca^{2+} signatures in seedlings. Cellular Ca^{2+} dynamics and relationship to Aequorin-based Ca^{2+} recording were explored using a GFP-based Ca^{2+} indicator, which suggested that a synchronous cellular Ca^{2+} signal is responsible for cold-induced Ca^{2+} response in seedlings, whereas asynchronous Ca^{2+} oscillation contributes to osmotic stress-induced Ca^{2+} increase in seedlings. The optimized recording system would be a powerful tool for the identification and characterization of novel components in Ca^{2+}-mediated stress-signaling pathways.

Key words: Aequorin; Case12; abiotic stress; calcium; *Arabidopsis*.

INTRODUCTION

Calcium ion has been adopted as a primary signal element during evolution. To respond to changing developmental and environmental cues, plant cells rapidly change cytosolic free Ca^{2+} concentration in time and space. The spatiotemporal patterning of cellular Ca^{2+} dynamics has been formulated as a concept of Ca^{2+} signature. Ca^{2+} signature, namely the alterations in amplitude, duration, frequency, and spatial distribution of Ca^{2+} signal, encodes information of the type and the strength of the stimuli (Knight et al., 1996; Webb et al., 1996; McAinsh and Hetherington, 1998; Trewavas and Malho, 1998). Such Ca^{2+}-encoded stimulus-specific information is decoded by downstream effectors. Most downstream effectors are Ca^{2+} sensing proteins, which bind to Ca^{2+} to initiate or regulate biochemical processes and ultimately translate information into specific end responses (Harper et al., 2004; Kim et al., 2009; Luan, 2009; DeFalco et al., 2010; Kudla et al., 2010). Therefore, the specificity of stimulus–response coupling is believed to be achieved by stimulus-defined Ca^{2+} encoding and decoding processes.

Ca^{2+} signaling regulates diverse cellular responses to abiotic and biotic stresses, plant hormones, light, and mechanical stimulation (Kudla et al., 2010). However, it remains unknown how plant cells generate stimulus-specific Ca^{2+} signals. A number of Ca^{2+}-signaling components have been identified in plant cells that comprise Ca^{2+}-signaling toolkits (Harper, 2001; McAinsh and Pittman, 2009; Kudla et al., 2010). Such cellular Ca^{2+}-signaling toolkits enable the cell to use both extracellular and internal sources of Ca^{2+}. However, in plant cells, most Ca^{2+} channels that control the entry of extracellular Ca^{2+} or the release of Ca^{2+} from internal store are still largely unidentified. So far, three families of proteins have been demonstrated to have Ca^{2+}-influx activity. Ligand-gated receptors, cyclic nucleotide-gated channels (CNGCs), and glutamate receptor-like channels (GLRs) have been shown to possess Ca^{2+}-influx activities. CNGCs function in defense signaling and thermosensing (Ali et al., 2007; Ma and Berkowitz, 2011; Finka et al., 2012), whereas GLRs are proposed to be responsible for selected amino acid-triggered Ca^{2+} influx, functioning in pollen tube growth (Michard et al.,

[1] To whom correspondence should be addressed. J.-K.Z. E-mail jkzhu@purdue.edu, tel. 765–496–7601, fax 765–494–0391. X.Z. E-mail zhu148@purdue.edu, tel. 765–496–7603, fax 765–494–0391.

doi:10.1093/mp/sst013, Advance Access publication 31 January 2013

Received 3 December 2012; accepted 15 January 2013

2011), stomatal closure (Cho et al., 2009), root development (Li et al., 2006; Qi et al., 2006), and defense signaling (Kwaaitaal et al., 2011; Vatsa et al., 2011). Unlike CNGCs and GLRs, two pore channel (TPC1) is a vacuolar Ca^{2+} release channel, regulating ABA-sensitive germination and stomatal opening (Peiter et al., 2005; Islam et al., 2010; Hedrich and Marten, 2011). In addition to the Ca^{2+}-influx system mentioned above, electrophysiological studies have shown Ca^{2+} currents when plasma membrane is hyperpolarized or depolarized, indicating the existence of voltage-gated Ca^{2+} channels in plants. In addition, the ligands 1,4,5-trisphosphate and cyclic ADP-ribose likely trigger Ca^{2+} release from internal stores through ligand receptor-operated channels in plants (Allen et al., 1995; Martinec et al., 2000; Navazio et al., 2000; Lemtiri-Chlieh et al., 2003), although the molecular identities of these channels have yet to be identified. On the other hand, most Ca^{2+} pumps and exchangers that rapidly transport cytosolic Ca^{2+} back to the extracellular space or internal membrane stores have been well characterized. Two types of Ca^{2+} pumps and exchangers, P-type Ca^{2+} ATPase (ECAs, ER-type Ca^{2+} ATPase and ACAs, autoinhibited Ca^{2+} ATPase) and Ca^{2+} exchanger (CAXs), are located in the plasma membrane and different organelles (Sze et al., 2000; Mäser et al., 2001; Shigaki and Hirschi, 2006). They bring Ca^{2+} to the resting level and are important in shaping Ca^{2+} signatures (McAinsh and Pittman, 2009).

Unveiling the mechanism by which plant cells initiate stimulus-specific Ca^{2+} signals is crucial to understanding how plants perceive and transduce signals to adapt to various stresses. A precise measurement of cellular Ca^{2+} dynamics is a prerequisite for identifying genes and defining their functions in Ca^{2+} signaling. So far, the measurements of Ca^{2+} dynamics at the cellular or whole plant level are performed in various plant species using different Ca^{2+} indicators, including ratiometric fluorescent dyes and genetically encoded Ca^{2+} indicators (Campbell et al., 1996; Knight et al., 1996, 1997; Cessna et al., 1998; Gong et al., 1998; Mori et al., 1998; Blume et al., 2000; Allen et al., 2001; Kosuta et al., 2008; Monshausen et al., 2009; Krebs et al., 2011; Munemasa et al., 2011; Ranf et al., 2012). However, stimuli-specific Ca^{2+} signatures have not been systematically defined in *Arabidopsis* at the level of either the single cell or the whole plant. Furthermore, the identification of the components, especially Ca^{2+}-influx channels and their regulators in Ca^{2+}-signaling toolkits, necessitate well-designed genetic screens in *Arabidopsis*.

To bridge these gaps, we developed an Aequorin-based FAS Ca^{2+} recording system that allows a systematic comparison of Ca^{2+} dynamics in response to stimuli of various strengths and types, including abiotic and biotic stresses, plant hormones, and amino acids in *Arabidopsis* seedlings. Using the GFP-based Ca^{2+} indicator Case12, we demonstrated cellular Ca^{2+} dynamics in response to cold and osmotic stresses, and provided experimental evidence that the whole seedling or organ-level Ca^{2+} patterns reflect combined single-cell Ca^{2+} dynamics of populations of cells. We further demonstrated that the FAS recording was able to detect alterations of Ca^{2+} signals by Ca^{2+} channel blockers. As a result, FAS recording could be a powerful system for the isolation of mutants with altered stimulus-specific Ca^{2+} signals, which may help reveal the molecular identities of Ca^{2+}-signaling components that are important in abiotic stress-signaling pathways.

RESULTS

Aequorin-Based FAS Recording for Tracking Spatiotemporal Ca^{2+} Signals in *Arabidopsis* Seedlings

In order to simultaneously monitor tissue-specific Ca^{2+} responses in multiple *Arabidopsis* seedlings, we developed an Aequorin-based FAS luminescence recording system. We used transgenic *Arabidopsis* plants expressing cytosolic Aequorin, referred to as the Aeq or Aeq wild-type plants. Aeq seedlings were grown vertically on MS agar in a square Petri dish at a density of about 100 seedlings per plate until 7 d old, and were then transferred onto an adhesive-backed film. A sheet of FAS was incubated with h-CTZ for the reconstitution of Aequorin. Stimuli-induced Ca^{2+} signals in FAS were recorded using a photon-counting camera (Supplemental Figure 1). Sequential luminescence images over the time course are shown in Figure 1, which demonstrate spatiotemporal dynamic changes of Ca^{2+} in response to different abiotic stress stimuli. The free cytosolic Ca^{2+} level in the cell is correlated with the luminescence intensity emitted from Aequorin (Gilroy et al., 1989). A comparison of the amplitude and duration of Ca^{2+} increase is made based on the average photon density, namely total photon density divided by the area of region of interest (ROI). As shown in Figures 1 and 2, abiotic stress stimuli-induced Ca^{2+} signals vary greatly in terms of the speed of signal initiation, and signal amplitude and duration, in addition to differences in tissue distribution patterns. In all cases, the amplitude, but not always the duration, of Ca^{2+} signals was correlated with the strength of the stimulus. For example, the 0°C water-induced Ca^{2+} amplitude was 1.4-fold higher than that induced by 4°C water. However, the duration of Ca^{2+} increase was the same under 0°C or 4°C, and both Ca^{2+} signals show only one sharp spike. In contrast, heat stress triggered a longer duration of Ca^{2+} increase, although the Ca^{2+} amplitudes were very similar to that triggered by 4°C water. As shown in Figures 1 and 2, seedlings responded differently to different levels of acidic pH. A delayed initiation of Ca^{2+} signals was observed in response to both pH 3.5 and pH 4.5 acidic stimuli, but the stronger acidic stimulus (pH 3.5) initiated an earlier and greater Ca^{2+} increase than the more moderate acidic stimulus (pH 4.5). In this study, mannitol, hydrogen peroxide, and sodium chloride were used for mimicking osmotic, oxidative, and salt stress stimuli, respectively. The concentrations used in this study were much lower than those used in previously published studies, which indicates a high sensitivity of our FAS recording. The lowest concentrations tested here for mannitol, NaCl, and hydrogen peroxide were 200, 50, and 1 mM, in which Ca^{2+} signals were

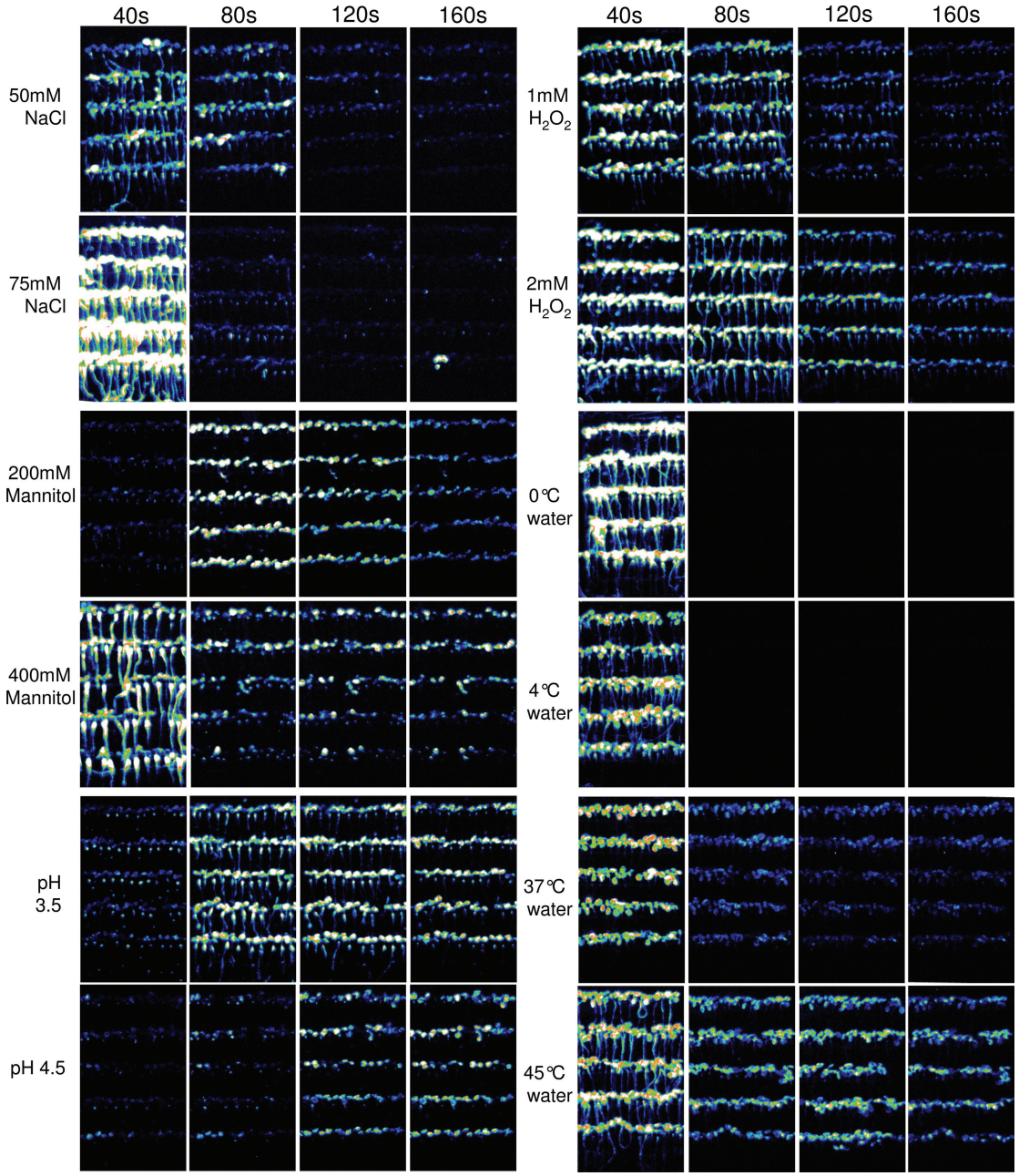

Figure 1. Abiotic Stress-Induced Spatiotemporal Patterns of Ca^{2+} Signals in *Arabidopsis* Seedlings.
Time course of luminescence images of FAS. Sequential images were collected using a photon-counting camera with an interval of 40-s photon-counting integrations upon application of stimuli. The type and strength of abiotic stress stimuli are indicated on the left of each panel, and time points are indicated on the top of each panel. The display range is 100–200 for all images.

clearly detectable, although the amplitudes were 2.5-, 1.4-, and 1.06-fold lower than those triggered by 400, 75, and 2 mM NaCl, mannitol, and H_2O_2, respectively. The results indicated that the Ca^{2+} amplitudes in whole seedlings were correlated with the strengths of osmotic, oxidative, and salt stresses (Figure 2). Interestingly, various tissue patterns of Ca^{2+} dynamics were observed, and the tissue patterns were not only related to the type, but also to the strength, of the stress stimuli. Moderate cold and heat stresses, such as 4°C and 37°C water, triggered strong Ca^{2+} signals in leaves, but they triggered only weak Ca^{2+} signals in roots. In contrast, severe cold and heat stress, such as 0°C and 45°C water, triggered strong Ca^{2+} signals in roots, in addition to the leaves. Such tissue-specific patterns were even more pronounced in the seedlings responding to the osmotic stress agent mannitol, in which Ca^{2+} signal in roots was not even detectable in response

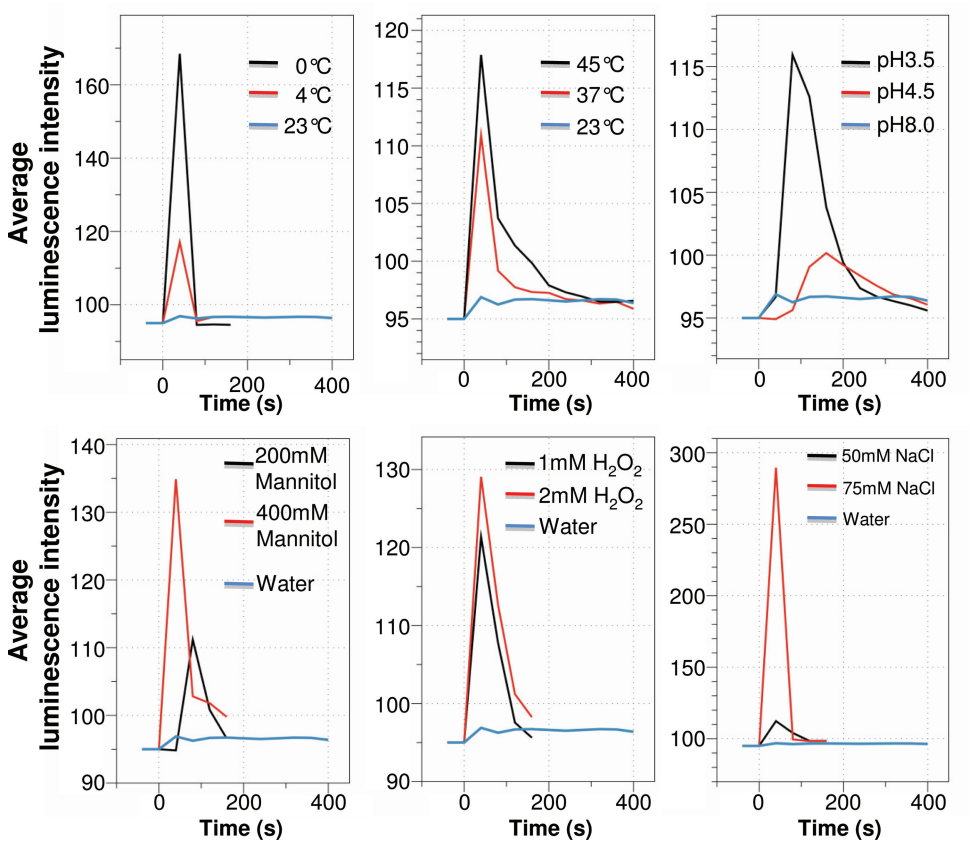

Figure 2. Temporal Patterns of Abiotic Stress Stimulus-Induced Ca^{2+} Signal of the Whole Seedlings.
Stimulus-induced Ca^{2+} increases are illustrated by the averaged photon intensity over time. The total photon was counted for 160 s for cold (0°C and 4°C water), oxidative (1 and 2 mM H_2O_2), osmotic (200 and 400 mM mannitol), and salt (50 and 75 mM NaCl) stress stimuli, and 400 s for heat (37°C and 45°C water), acidic (pH 3.5 and 4.5) stress stimuli, and control (room temperature water, pH 7.6).

to 200 mM mannitol (Figure 1). The speed of initiation of Ca^{2+} signal was also correlated with the strength of the stimuli, as exemplified by delayed responses to 200 mM mannitol and pH 4.5, compared to the responses to 400 mM mannitol and pH 3.5 medium, respectively.

Taken together, the Aequorin-based FAS recording system provided a platform for a highly sensitive and robust Ca^{2+} signal recording. Such Ca^{2+} recording revealed diverse abiotic stress stimuli-specific Ca^{2+} spatiotemporal patterns of Ca^{2+} signals.

A GFP-Based Ca^{2+} Indicator for Monitoring Cellular Ca^{2+} Dynamics

Aequorin-recorded Ca^{2+} signal is a readout of populations of cells. It is unclear how Aequorin-recorded Ca^{2+} signature in whole seedlings or tissues of seedlings is related to cellular Ca^{2+} dynamics. To understand cellular Ca^{2+} dynamics underlying the FAS-recorded Ca^{2+} signature, we used a genetically encoded Ca^{2+} indicator, Case12, for tracking cellular Ca^{2+} dynamic changes in response to cold and osmotic stresses. Case12 is a GFP-based Ca^{2+} indicator, for which changes in fluorescent intensity are directly correlated with changes in Ca^{2+} concentration (Souslova et al., 2007; Zhu et al., 2010). In this study, we generated transgenic *Arabidopsis* plants constitutively expressing Case12 in the cytosol. Ca^{2+} signals in the root cells were recorded upon application of 0°C water or 400 mM mannitol under a confocal microscope. As shown in Figure 3A and 3B, 0°C water triggered synchronous Ca^{2+} spikes in root cells (Supplemental Movie 1). The amplitude and duration of 0°C water-induced Ca^{2+} spikes were various among single cells, and the average amplitude and duration were 218.54 ± 53.67 and 19.27 ± 1.98 s, respectively. In contrast, as shown in Figure 3C and 3D, mannitol-induced Ca^{2+} oscillations in most cells (Supplemental Movie 2) have an average frequency of 39.95 ± 15.07 s. The average amplitude and duration of mannitol-induced Ca^{2+} spike were 60.44 ± 21.66 and 17.28 ± 1.54 s, respectively, which were lower than that of 0°C water-induced Ca^{2+} spikes. It appears that the amplitudes and frequencies varied while the durations were similar among cold and mannitol-induced Ca^{2+} spikes. Overall, there were great differences in cold and osmotic stress stimuli-induced single-cell Ca^{2+} dynamics. Our results suggest that Aequorin-based FAS-recorded Ca^{2+} signals in response to cold and osmotic stress stimuli reflect distinct cellular Ca^{2+} dynamics under the different stimuli. Synchronous Ca^{2+} spikes contributed to cold induced overall Ca^{2+} increase in the root, whereas osmotic stress stimulus induced overall Ca^{2+} changes

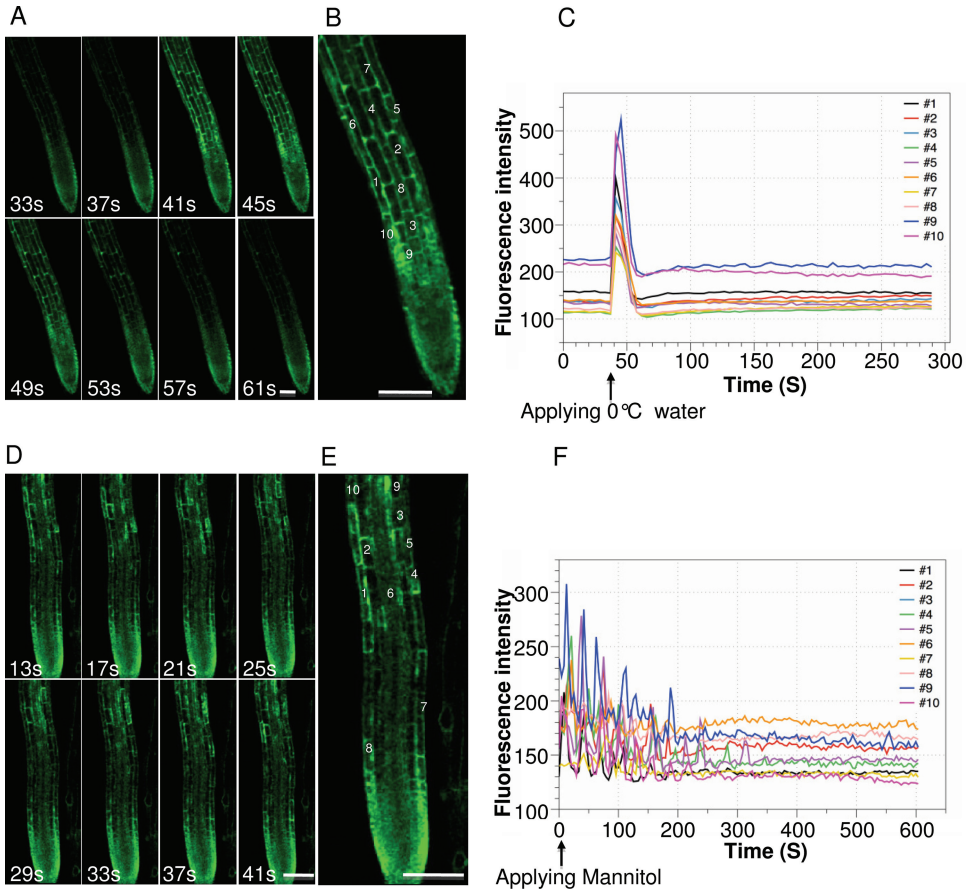

Figure 3. Cellular Ca^{2+} Dynamics in *Arabidopsis* Root Cells.
(A) Selected time series of images of 0°C water treated root of 5-day-old CaFP300 seedling. Time points are indicated on the bottom of each panel.
(B) Enlarged image of root cells showing a Ca^{2+} response to 0°C water. The responsive cells are indicated by the numbers.
(C) Changes in fluorescence intensity of the single cells responding to 0°C water over the time course. Colored lines tagged by the numbers represent corresponding cells in the root as indicated in (B).
(D) Selected time series of images of 400 mM mannitol treated root of 5-day-old CaFP300 seedlings. Time points are indicated on the bottom of each panel.
(E) Enlarged image of root cells showing a Ca^{2+} response to 400 mM mannitol. The responsive cells are indicated by the numbers.
(F) Changes in fluorescence intensity of the single cells responding to 400 mM mannitol over the time course. Colored lines represent corresponding cells in the root as indicated in (E).

in the root were attributed to asynchronous Ca^{2+} oscillations in individual root cells.

FAS Recording for Monitoring Ca^{2+} Response of *Arabidopsis* Seedlings to Hormones, Pathogen Elicitor, and Amino Acids

Aiming at adapting the FAS system for a simple, highly sensitive, and robust approach for recording Ca^{2+} response to any given stimuli, we further evaluated the use of the FAS system in recording Ca^{2+} signals in response to a number of stimuli, including the plant hormones salicylic acid (SA), Jasmonic acid (JA), Abscisic acid (ABA), and brassinosteriod (BR), the pathogen elicitor flagellin, and the amino acids L-glutamate, L-glycine, L-cystine, L-alanine, L-serine, and L-aspargine. As shown in Figure 4, 180 μM SA and 450 μM JA, the lowest concentrations tested in this study, induced Ca^{2+} increases that could be visualized by FAS recording. The highest amplitudes of SA- and JA-induced Ca^{2+} signals occurred in the second or third 40 s, depending on the concentration of SA and JA. High concentrations of SA triggered earlier and higher Ca^{2+} response than low concentrations of SA, indicating that the initiation and amplitude, but not the duration, of SA-induced Ca^{2+} were closely related to SA concentration. Interestingly, it appeared that the roots were more sensitive to SA, which was evident by the initial strong and prolonged Ca^{2+} signals induced by SA in roots. In contrast, JA-induced Ca^{2+} signals were relative weak, and were detected mostly in leaves. No significant differences in the initiation and amplitude of Ca^{2+} responses were observed in response to low and high concentrations of JA. ABA- and BR-induced Ca^{2+} signals could not be detected in 7-day-old seedlings at the highest concentration of 20 μM ABA and 2 μM BR tested in this study (data not shown). However, prolonged Ca^{2+} increases were observed in the leaves of 14-day-old seedlings in response to

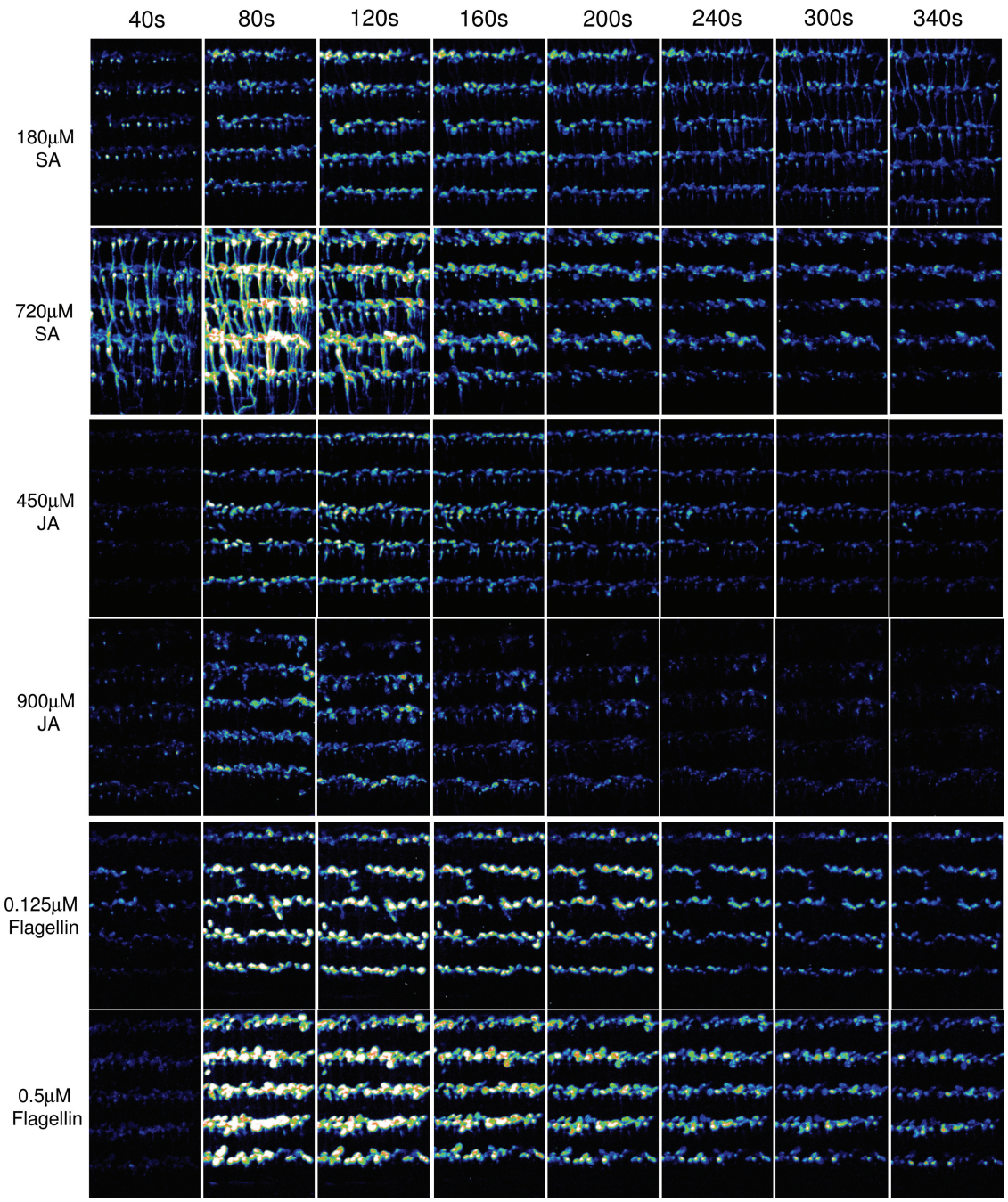

Figure 4. Spatiotemporal Ca^{2+} Responses of *Arabidopsis* Seedlings to Plant Hormones and Pathogen Elicitor.
Sequential integrated luminescence images of FAS over the time course upon application of SA, JA, and flagellin. The type and concentration of the stimuli are indicated on the left of each panel, and time points are indicated on the top of each panel. The display range is 100–200 for all images.

7 μM ABA and 1 μM BR. The highest amplitudes varied greatly among the leaves of 14-day-old seedlings in response to SA, JA, ABA, and BR, as shown in Supplemental Figure 2.

Similarly, FAS recording revealed that flagellin induced prolonged Ca^{2+} increases that were mostly detected in the leaves, showing a tissue-specific sensing of the pathogen elicitor (Figure 4). The lowest concentration of flagellin used in this study was 0.125 μM, which still induced clearly detectable Ca^{2+} increases. Flagellin at 0.5 μM induced a Ca^{2+} signal with a higher amplitude and longer duration compared to that induced by 0.125 μM flagellin. Six amino acids have been considered to be agonists of GRL3.3-mediated Ca^{2+} influx (Qi et al., 2006). We visualized Ca^{2+} response to these six amino acids using FAS recording. As shown in Figure 5, all six amino acids induced strong Ca^{2+} responses during the first 40 s, and the amplitudes were correlated with the concentrations. The

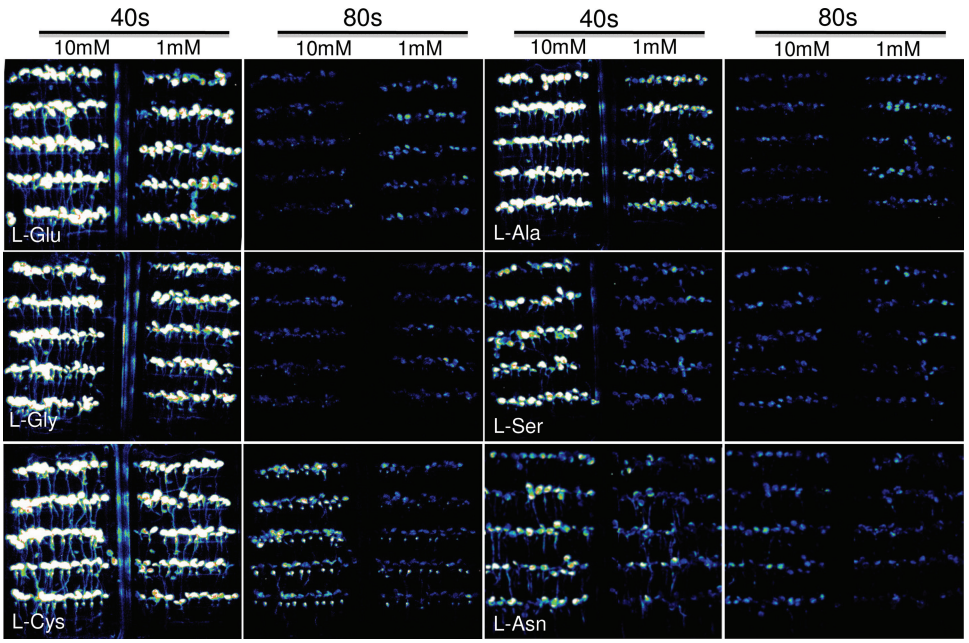

Figure 5. Spatiotemporal Ca^{2+} Responses of *Arabidopsis* Seedlings to Amino Acids.
Integrated luminescence images of FAS at first and second 40 s upon application of amino acids. Amino acids are indicated in the first 40 s integrated images, and the concentration of amino acids and the time points are indicated on the top of each panel.

highest Ca^{2+} amplitude was observed for L-cystine, and the lowest one was for L-asparigine (Table1). The order of Ca^{2+} amplitude induced by each amino acid was very similar to that reported previously with the same concentration using a luminometer which is supposed to be more sensitive than imaging (Qi et al., 2006). The results suggest that our FAS Ca^{2+} recording is highly sensitive and reliable.

FAS Recording Reveals Tissue-Specific Ca^{2+} Responses to Metal Ions

We chose two heavy metal ions, Cu^{2+} and Cd^{2+}, as the other stress stimuli to examine the spatiotemporal patterns and sources of metal ion-triggered Ca^{2+} signals. It has been unclear whether these two metal ions can trigger Ca^{2+} signals in *Arabidopsis*. Only recently, it has been reported that Cu^{2+} ion could activate ER Ca^{2+} channels in the marine algae *Ulva compressa* to release Ca^{2+} from the ER (Gonzalez et al., 2010). Ruthenium Red (RR) and neomycin are membrane-permeable Ca^{2+} channel blockers that predominantly inhibit ryanodine receptors (RYRs)-like intracellular Ca^{2+} channels and Ca^{2+} release through IP3-regulated Ca^{2+} channels, respectively. Gadolinium (Ga^{3+}) has been widely used as a plasma membrane Ca^{2+} channel blocker to inhibit Ca^{2+} influx from the extracellular space (Tracy et al., 2008). To examine the effect

Table 1. Ca^{2+} Response of *Arabidopsis* Seedlings to Amino Acids.

Amino acid	L-Glu		L-Gly		L-Cys	
Time/conc.	10 mM	1 mM	10 mM	1 mM	10 mM	1 mM
40 s	157.59 ± 16.61	120.67 ± 6.32	161.21 ± 2.54	127.34 ± 4.32	177.09 ± 11.07	141.44 ± 5.32
80 s	93.78 ± 3.41	94.45 ± 2.56	93.71 ± 2.14	93.59 ± 1.02	99.99 ± 1.15	94.76 ± 2.14
120 s	92.79 ± 2.11	94.13 ± 1.34	92.93 ± 2.33	93.06 ± 0.59	93.64 ± 1.05	93.62 ± 1.12
160 s	92.65 ± 1.05	94.31 ± 0.89	92.83 ± 1.09	93.13 ± 0.89	92.28 ± 0.75	92.68 ± 0.98
Amino acid	L-Ala		L-Ser		L-Asn	
Time/conc.	10 mM	1 mM	10 mM	1 mM	20 mM	10 mM
40 s	158.95 ± 8.97	102.85 ± 5.43	110.39 ± 5.69	94.42 ± 1.03	101.57 ± 5.33	96.26 ± 2.64
80 s	93.55 ± 3.59	94.59 ± 2.12	93.41 ± 2.06	93.22 ± 1.12	94.22 ± 2.08	93.32 ± 3.15
120 s	92.87 ± 1.33	93.76 ± 1.45	92.38 ± 1.08	92.70 ± 0.23	92.15 ± 1.13	92.12 ± 2.08
160 s	92.92 ± 0.16	94.06 ± 0.32	92.20 ± 1.15	92.79 ± 0.43	91.87 ± 1.08	91.67 ± 1.10

Note: values are the average photon intensity ± SD of three independent experiments.

of blocking Ca^{2+} entry or release on potential Cu^{2+}- and Cd^{2+}-induced Ca^{2+} signals, we compared Ga^{2+}, RR, and Neomycin-treated and -untreated FAS recording in response to Cu^{2+} and Cd^{2+}. Images of Ca^{2+} channel blocker-untreated and -treated FAS were acquired simultaneously upon application of Cu^{2+} and Cd^{2+}. As shown in Figure 6 and Supplemental Figure 3, both Cu^{2+} and Cd^{2+} induced strong and prolonged Ca^{2+} increases in leaves, whereas Ca^{2+} signals in roots were undetectable. Compared to Cu^{2+}, Cd^{2+} initiated Ca^{2+} signal later but with a longer duration (Figure 6C and 6D). Application of Ga^{2+} reduced Cu^{2+} and Cd^{2+}-induced Ca^{2+} amplitude by approximately 92% and 94%, respectively, indicating that Cu^{2+} and Cd^{2+} trigger Ca^{2+} increase mostly by activating Ca^{2+} influx through the plasma membrane. In the case of Cu^{2+}, RR and neomycin reduced Ca^{2+} amplitude by 49% and 66%, respectively. However, RR almost abolished Ca^{2+} signals after 280 s (Figure 6A and Supplemental Figure 3A). Similarly, RR and neomycin also greatly inhibited Cd^{2+}-induced Ca^{2+} signal, reducing the amplitude by 64% and 79%, respectively. We found that neomycin initially enhanced Cu^{2+} and Cd^{2+}-induced Ca^{2+} signals at the first 40 s (Figure 6B and Supplemental Figure 3B), which is similar to observations reported previously (Tracy et al., 2008).

Taken together, our results show that Cu^{2+} and Cd^{2+} induced strong Ca^{2+} signals specifically in leaves. The FAS-recorded spatiotemporal patterns of these two divalent metal ion-induced Ca^{2+} signals are different from the patterns induced by the other abiotic stress stimuli. It appears that Cu^{2+} and Cd^{2+} initiate Ca^{2+} signals by activating Ca^{2+} influx across the plasma membrane. Because internal Ca^{2+} channel blockers also significantly reduced Cu^{2+}- and Cd^{2+}-induced Ca^{2+} signals, Ca^{2+} release from internal stores may also play a role in Ca^{2+} signaling in *Arabidopsis*.

DISCUSSION

Genetically encoded Ca^{2+} indicators have been perfected to meet the needs of accurate measurement of Ca^{2+} dynamics in cells. Aequorin (McCombs and Palmer, 2008), an early version of Ca^{2+} indicator, contributed to the formulation of the concept of Ca^{2+} signature in plants (Knight et al., 1991). However, low photon production and less-than-robust measurement have hindered the use of Aequorin in high-resolution Ca^{2+} imaging and genetic screens in plants (Plieth, 2001). In this study, we revisited Aequorin and developed an Aequorin-based FAS luminescence Ca^{2+} recording system in *Arabidopsis*. Using the FAS recording system, we compared various stimuli, including abiotic and biotic stresses, hormones, and amino acids in their induction of Ca^{2+} responses in *Arabidopsis* seedlings. The FAS Ca^{2+} recording revealed tissue-specific Ca^{2+} signatures that are associated with the type and strength of stimuli. To our knowledge, such a systematic comparison, which is important for the concept of Aequorin-recorded Ca^{2+} signatures, has not been made in the *Arabidopsis* model plant previously. The optimized FAS recording system may also enable a high-throughput genetic screen for the identification of potentially novel Ca^{2+}-signaling components in stress responses. Therefore, the FAS system can be a useful tool for studying Ca^{2+} signaling in *Arabidopsis* plants.

The non-invasive Case12-based Ca^{2+} recording revealed the complexity of cellular Ca^{2+} dynamics in individual living cells. The readout of FAS recording represents the averaged signals from cell populations, which masks the behavior of individual cells. In many cases, such as under osmotic, oxidative, and salt stresses, there are unsynchronized Ca^{2+} oscillations or transients in individual cells. This cellular heterogeneity in Ca^{2+} oscillations could be overcome by cold stress. Thus, FAS-recorded Ca^{2+} signal in cold stress-treated seedlings represent the collective behavior of synchronized Ca^{2+} oscillations in single cells. The observations imply that different cellular machinery in the cell is responsible for responding to different stimuli. Unsynchronized cellular Ca^{2+} dynamics could originate from cell-specific Ca^{2+}-signaling toolkits that are regulated by the stimuli, and may also be attributed to cell–cell communication and the accessibility of individual cells to the stimuli. Mathematic simulations of oscillatory behaviors of cell populations suggested that Aequorin-recorded Ca^{2+} increases results from in-phase oscillations whereas the Ca^{2+} decrease is due to the out-phase oscillation of cell populations (Dodd et al., 2006; Plieth, 2010; Batistic and Kudla, 2012). However, our results suggest that such models of Ca^{2+} signaling may not be applicable to diverse stimulus-specific Ca^{2+} dynamics. In addition, experiments with Ca^{2+} channel blockers suggested that Aequorin-recorded initial Ca^{2+} increase is attributed to single-cell Ca^{2+} amplitudes in which both in-phase or out-phase oscillations might occur. In the present study, we could not correlate the Case12 recording of cellular Ca^{2+} dynamics with FAS recording of tissue-level Ca^{2+} dynamics in response to a given stimulus due to a lack of mutants that express both Ca^{2+} indicators. Nevertheless, we observed the effects of Ca^{2+} channel blockers on Ca^{2+} signals at the tissue level, suggesting that FAS-recorded signals are relevant to Ca^{2+} dynamic changes at the cellular level.

Aequorin-recorded Ca^{2+} dynamics to a great extent depends on not only the sensitivity of the assay system, but also the state of the plants. For the FAS system, 7-day-old seedlings are ideal for detecting Ca^{2+} responses of both roots and leaves to most stimuli tested in this study. However, for some stimuli that are known to trigger Ca^{2+} responses in the leaves, such as the plant hormones ABA and BR, the pathogen elicitor flagellin and heavy metal ions, characterization of Ca^{2+} responses or screening for the mutants with altered Ca^{2+} responses would ideally be conducted in older seedlings. The high sensitivity and robustness are also a prerequisite for high-throughput screens. In particular, the high sensitivity of the system allows the use of relatively mild stress stimuli for triggering Ca^{2+} responses. Severe stress treatments likely

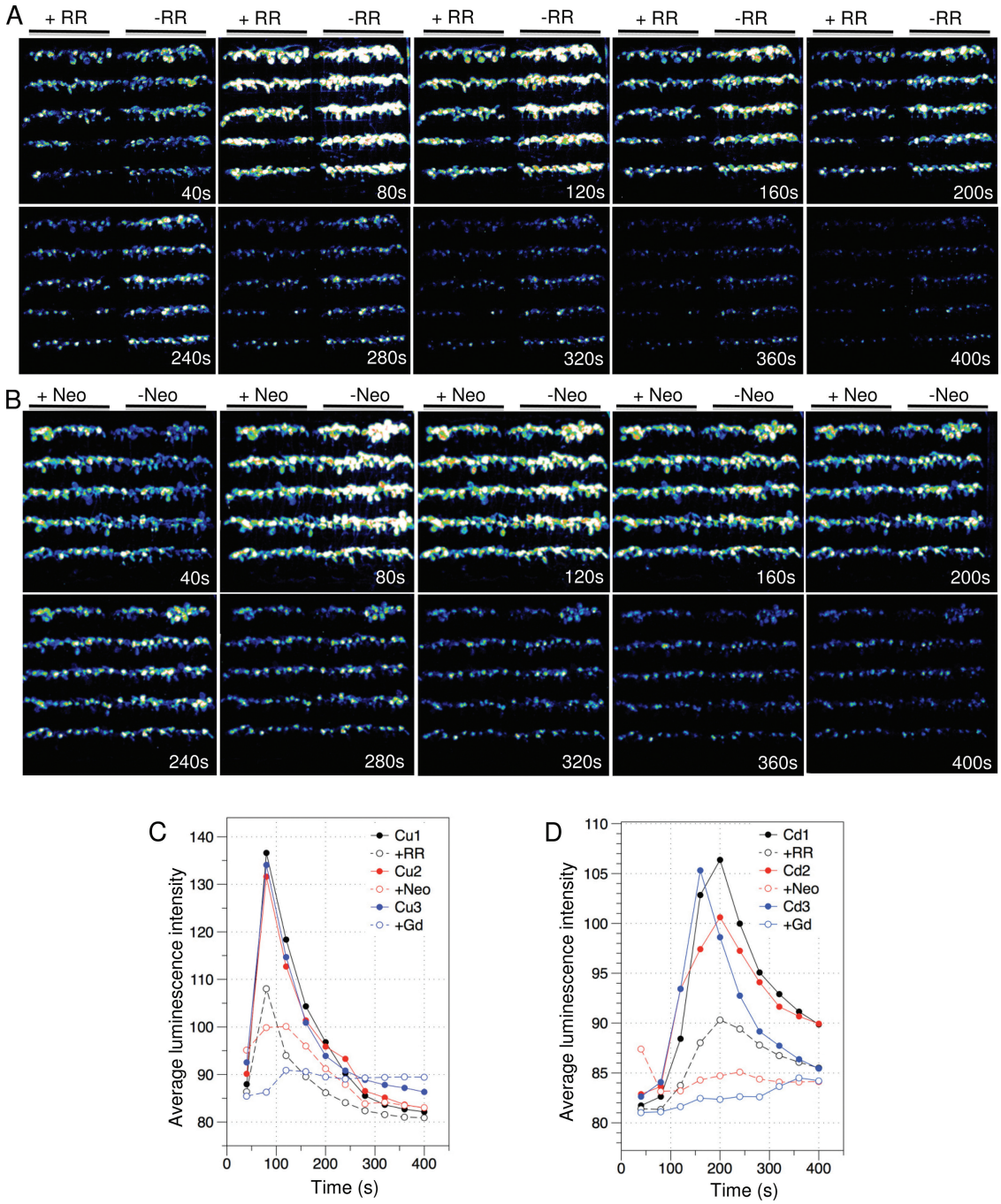

Figure 6. Cu^{2+} and Cd^{2+}-Induced Ca^{2+} Signals in the Leaves of *Arabidopsis* Seedlings.
(A, B) Effect of 100 µM RR and 600 µM neomycin on Cu^{2+}-triggered Ca^{2+} increase. Time series of integrated luminescence images of FAS were collected with an interval of 40-s photon-counting integrations upon application of 10 mM $CuCl_2$. Time points are indicated on each image panel. 100 µM RR (A) and 600 µM neomycin (B)-treated and -untreated FAS are indicated on the top of each panel.
(C, D) Temporal pattern of effects of RR, neomycin and Ga^{3+} on Cu^{2+} (C) and Cd^{2+} (D)-induced Ca^{2+} increases. Changes of the averaged photon intensity over times are indicated by the colored lines with open circles for RR, neomycin, and Ga^{3+} treatments, and the same colored lines with solid circles are corresponding controls treated with only $CuCl_2$ and $CdCl_2$.

cause damage to the cells, leading to more artifacts. For all stimuli tested in this study, the FAS system was able to image Ca^{2+} responses to the stimuli applied at levels used for Ca^{2+} reading by luminometers (Knight et al., 1997; Kawano et al., 1998; Tracy et al., 2008; Munemasa et al., 2011; Pan et al., 2012; Ranf et al., 2012), which normally is more sensitive than Ca^{2+} luminescence imaging. Therefore, the FAS system has advantages over other systems reported previously not only

for its highly sensitive Ca^{2+} recording, but also for its detection of spatial Ca^{2+} responses.

In conclusion, the Aequorin-based FAS system developed in this study provides a powerful tool for studying Ca^{2+} signaling in response to various stimuli. Importantly, the FAS system offers a platform for future identification of Ca^{2+}-signaling components in stress-signaling pathways. In combination with other techniques, the FAS system would become a very useful tool for studying the specificity and crosstalk in plant-signaling networks.

METHODS

Plant Material and Growth Conditions

The *Arabidopsis thaliana* Col-0-expressing cytosolic Aequorin (referred to as Aeq wild-type) was obtained from Dr Marc R. Knight (Knight et al., 1991). Seedlings were grown in the growth chamber conditioned with a standard light–dark cycle of 16 h of light and 8 h of dark at 23°C. Ca^{2+} indicator Case12 (Souslova et al., 2007) constructed in a binary vector was introduced into *Arabidopsis* ecotype Col-0 by Agrobacterium-mediated transformation. An independent transgenic line, CaFP300, expressing a high level of Case12 was used in this study.

Establishment of Aequorin-Based FAS Luminescence Recording System

For establishing FAS system, Aeq wild-type seeds were planted in a square plate (10 × 10 cm square Petri dish with grid, Fisher Scientific, USA) containing full- strength MS medium, 1% sucrose, and 1.2% agar. Aeq seedlings were grown vertically on the plate at a density of about 100 seedlings per plate and transferred onto a clear adhesive film (Adhesive PCR Plate Seals, Thermo Scientific, USA) on the seventh day after germination. A sheet of FAS (about 100 seedlings) was incubated in the plate containing 15 ml water and 30 μg h-CTZ (coelenterazine, NanoLight Technolgies, Arizona, USA) for 5 h overnight for reconstitution of Aequorin.

Aequorin Luminescence Imaging and Analysis

A sheet of FAS was placed on the stage of the luminescence imaging system (Princeton Instruments, New Jersey, USA) and images were acquired immediately upon application of stimuli. The time gap between applying stimuli and recording image was about 2–4 s. For EMS screening, two integrated images were collected at first and second 40 s. For other experiments, the time series of Ca^{2+} recording was as indicated in the figures or figure legends. Qualitative analysis of luminescence images was performed using ImageJ. An average photon intensity of stimulus-induced luminescence signals at any given time was defined as the total photon intensity of luminescence signals emitted by FAS divided by the area of ROI. Plant hormones, SA, JA, and ABA were dissolved in 100% ethanol, whereas eBL was dissolved in DMSO. Therefore, a negative control of ethanol or DMSO in the same final concentrations as in the working solution of hormones was included in hormone-induced Ca^{2+} response. The stocks of 1 mM flagellin and 100 mM amino acid were dissolved in water and pHs of the working solutions of these two stimuli were unadjusted. For pretreatments with Ca^{2+} channel blockers, the FAS sheets were cut and divided equally into two parts. Half of the FAS sheets were pretreated with 50 μM $GaCl_3$, 100 μM RR, or 600 μM neomycin in h-CTZ incubation solution for 20 min, respectively, while other half of the FAS sheets remained in the h-CTZ incubation solution without adding blockers. Treated and untreated FAS sheets were the assembled into one piece and imaged for 400 s with a 40-s interval of integration upon application of 10 mM $CuCl_2$ or 10 mM $CdCl_2$. For cam mutant analysis, Aeq wild-type and cam mutant seeds were planted on MS agar in the same plate with a similar density, occupying the left or the right half of the plate. Seven-day-old Aeq and cam seedlings were transferred onto an adhesive film and incubated with h-CTZ, and images were acquired for 160 s as described above. Stimuli-induced Ca^{2+} amplitudes were compared at the time point in which the highest Ca^{2+} amplitudes were observed. The highest Ca^{2+} amplitudes were normalized by total photon intensity of luminescence signals emitted from discharged FAS in the solution of 1 M $CaCl_2$ and 20% ethanol.

Confocal Ca^{2+} Imaging

Five-day-old seedlings of CaFP300 were placed in a customized chamber, which was created by placing a small piece of clay between a coverslip and a slide. A polyethylene tube (0.58 mm diameter, PerkinElmer, USA) was connected to a 1-ml syringe and the other end of the tube was fixed on the slide next to the chamber. Stimulus solution was slowly injected into the chamber just prior to acquiring images. For cold stimulus, CaFP300 seeds were directly planted in a chambered cover glass (Nalge Nunc International, USA) containing a thin layer of MS medium, and grown vertically for 5 d. 0°C water was added into the chamber just prior to acquiring images. Ca^{2+} imaging was performed using an inverted Nikon A1R confocal laser-scanning microscope with a 20× water immersion lens (numerical aperture 0.75). Time series images were collected at an interval of 4 s with excitation and emission wavelengths of 488 nm and 500–550 nm at a pixel resolution of 512 × 512. Data were exported and processed in DataGraph (Visual Data Tools Inc., Chapel Hill, North Carolina, USA).

SUPPLEMENTARY DATA

Supplementary Data are available at *Molecular Plant Online.*

FUNDING

This work was supported by National Institutes of Health grant R01GM059138 to J.-K.Z.

ACKNOWLEDGMENTS

We are grateful to B. Stevenson for technical assistance and Dr Marc R. Knight for providing Aequorin transgenic line. No conflict of interest declared.

REFERENCES

Ali, R., Ma, W., Lemtiri-Chlieh, F., Tsaltas, D., Leng, Q., von Bodman, S., and Berkowitz, G.A. (2007). Death don't have no mercy and neither does calcium: *Arabidopsis* CYCLIC NUCLEOTIDE GATED CHANNEL2 and innate immunity. Plant Cell. **19**, 1081–1095.

Allen, G.J., Chu, S.P., Harrington, C.L., Schumacher, K., Hoffmann, T., Tang, Y.Y., Grill, E., and Schroeder, J.I. (2001). A defined range of guard cell calcium oscillation parameters encodes stomatal movements. Nature. **411**, 1053–1057.

Allen, G.J., Muir, S.R., and Sanders, D. (1995). Release of Ca^{2+} from individual plant vacuoles by both InsP3 and cyclic ADP-ribose. Science. **268**, 735–737.

Batistic, O., and Kudla, J. (2012). Analysis of calcium signaling pathways in plants. Biochim. Biophys. Acta. **1820**, 1283–1293.

Blume, B., Nurnberger, T., Nass, N., and Scheel, D. (2000). Receptor-mediated increase in cytoplasmic free calcium required for activation of pathogen defense in parsley. Plant Cell. **12**, 1425–1440.

Campbell, A.K., Trewavas, A.J., and Knight, M.R. (1996). Calcium imaging shows differential sensitivity to cooling and communication in luminous transgenic plants. Cell Calcium. **19**, 211–218.

Cessna, S.G., Chandra, S., and Low, P.S. (1998). Hypo-osmotic shock of tobacco cells stimulates Ca^{2+} fluxes deriving first from external and then internal Ca^{2+} stores. J. Biol. Chem. **273**, 27286–27291.

Cho, D., Kim, S.A., Murata, Y., Lee, S., Jae, S.K., Nam, H.G., and Kwak, J.M. (2009). De-regulated expression of the plant glutamate receptor homolog AtGLR3.1 impairs long-term Ca^{2+}-programmed stomatal closure. Plant J. **58**, 437–449.

DeFalco, T.A., Bender, K.W., and Snedden, W.A. (2010). Breaking the code: Ca^{2+} sensors in plant signalling. Biochem. J. **425**, 27–40.

Dodd, A.N., et al. (2006). Time of day modulates low-temperature Ca signals in *Arabidopsis*. Plant J. **48**, 962–973.

Finka, A., Cuendet, A.F., Maathuis, F.J., Saidi, Y., and Goloubinoff, P. (2012). Plasma membrane cyclic nucleotide gated calcium channels control land plant thermal sensing and acquired thermotolerance. Plant Cell. **24**, 3333–3348.

Gilroy, S., Hughes, W.A., and Trewavas, A.J. (1989). A comparison between Quin-2 and Aequorin as indicator of cytoplasmic calcium levels in higher plant cell protoplasts. Plant Physiol. **90**, 482–491.

Gong, M., van der Luit, A.H., Knight, M.R., and Trewavas, A.J. (1998). Heat-shock-induced changes in intracellular Ca^{2+} level in tobacco seedlings in relation to thermotolerance. Plant Physiol. **116**, 429–437.

Gonzalez, A., Trebotich, J., Vergara, E., Medina, C., Morales, B., and Moenne, A. (2010). Copper-induced calcium release from ER involves the activation of ryanodine-sensitive and IP(3)-sensitive channels in Ulva compressa. Plant Signal Behav. **5**, 1647–1649.

Harper, J.F. (2001). Dissecting calcium oscillators in plant cells. Trends Plant Sci. **6**, 395–397.

Harper, J.F., Breton, G., and Harmon, A. (2004). Decoding $Ca^{(2+)}$ signals through plant protein kinases. Annu. Rev. Plant Biol. **55**, 263–288.

Hedrich, R., and Marten, I. (2011). TPC1–SV channels gain shape. Mol. Plant. **4**, 428–441.

Islam, M.M., Munemasa, S., Hossain, M.A., Nakamura, Y., Mori, I.C., and Murata, Y. (2010). Roles of AtTPC1, vacuolar two pore channel 1 in *Arabidopsis* stomatal closure. Plant Cell Physiol. **51**, 302–311.

Kawano, T., Sahashi 1, N., Takahashi, K., Uozumi, N., and Muto, S. (1998). Salicylic acid induces extracellular superoxide generation followed by an increase in cytosolic calcium ion in tobacco suspension culture: the earliest events in salicylic acid signal transduction. Plant Cell Physiol. **39**, 721–730.

Kim, M.C., Chung, W.S., Yun, D.J., and Cho, M.J. (2009). Calcium and calmodulin-mediated regulation of gene expression in plants. Mol. Plant. **2**, 13–21.

Knight, H., Trewavas, A.J., and Knight, M.R. (1996). Cold calcium signaling in *Arabidopsis* involves two cellular pools and a change in calcium signature after acclimation. Plant Cell. **8**, 489–503.

Knight, H., Trewavas, A.J., and Knight, M.R. (1997). Calcium signalling in *Arabidopsis thaliana* responding to drought and salinity. Plant J. **12**, 1067–1078.

Knight, M.R., Campbell, A.K., Smith, S.M., and Trewavas, A.J. (1991). Transgenic plant aequorin reports the effects of touch and cold-shock and elicitors on cytoplasmic calcium. Nature. **352**, 524–526.

Kosuta, S., Hazledine, S., Sun, J., Miwa, H., Morris, R.J., Downie, J.A., and Oldroyd, G.E. (2008). Differential and chaotic calcium signatures in the symbiosis signaling pathway of legumes. Proc. Natl Acad. Sci. U S A. **105**, 9823–9828.

Krebs, M., Held, K., Binder, A., Hashimoto, K., Den Herder, G., Parniske, M., Kudla, J., and Schumacher, K. (2011). FRET-based genetically encoded sensors allow high-resolution live cell imaging of Ca^{2+} dynamics. Plant J. **69**, 181–192.

Kudla, J., Batistic, O., and Hashimoto, K. (2010). Calcium signals: the lead currency of plant information processing. Plant Cell. **22**, 541–563.

Kwaaitaal. M., Huisman, R., Maintz, J., Reinstädler, A., and Panstruga, R. (2011). Ionotropic glutamate receptor (iGluR)-like channels mediate MAMP-induced calcium influx in *Arabidopsis thaliana*. Biochem. J. **440**, 355–365.

Lemtiri-Chlieh, F., MacRobbie, E.A., Webb, A.A., Manison, N.F., Brownlee, C., Skepper, J.N., Chen, J., Prestwich, G.D., and Brearley, C.A. (2003). Inositol hexakisphosphate mobilizes an endomembrane store of calcium in guard cells. Proc. Natl Acad. Sci. U S A. **100**, 10091–10095.

Li, J., Zhu, S., Song, X., Shen, Y., Chen, H., Yu, J., Yi, K., Liu, Y., Karplus, V.J., Wu, P., et al. (2006). A rice glutamate receptor-like gene is critical for the division and survival of individual cells in the root apical meristem. Plant Cell. **18**, 340–349.

Luan, S. (2009). The CBL–CIPK network in plant calcium signaling. Trends Plant Sci. **14**, 37–42.

Ma, W., and Berkowitz, G.A. (2011). Ca^{2+} conduction by plant cyclic nucleotide gated channels and associated signaling components in pathogen defense signal transduction cascades. New Phytol. **190**, 566–572.

Martinec, J., Feltl, T., Scanlon, C.H., Lumsden, P.J., and Machackova, I. (2000). Subcellular localization of a high affinity binding site for D-myo-inositol 1,4,5-trisphosphate from *Chenopodium rubrum*. Plant Physiol. **124**, 475–483.

Mäser, P., Thomine, S., Schroeder, J.I., Ward, J.M., Hirschi, K., Sze, H., Talke, I.N., Amtmann, A., Maathuis, F.J., Sanders, D., et al. (2001). Phylogenetic relationships within cation transporter families of *Arabidopsis*. Plant Physiol. **126**, 1646–1667.

McAinsh, M.R., and Hetherington, A.M. (1998). Encoding specificity in Ca^{2+} signalling systems. Trends Plant Sci. **3**, 32–36.

McAinsh, M.R., and Pittman, J.K. (2009). Shaping the calcium signature. New Phytol. **181**, 275–294.

McCombs, J.E., and Palmer, A.E. (2008). Measuring calcium dynamics in living cells with genetically encodable calcium indicators. Methods. **46**, 152–159.

Michard, E., Lima, P.T., Borges, F., Silva, A.C., Portes, M.T., Carvalho, J.E., Gilliham, M., Liu, L.H., Obermeyer, G., and Feijo, J.A. (2011). Glutamatereceptor-like genes form Ca^{2+} channels in pollen tubes and are regulated by pistil D-serine. Science. **332**, 434–437.

Monshausen, G.B., Bibikova, T.N., Weisenseel, M.H., and Gilroy, S. (2009). Ca^{2+} regulates reactive oxygen species production and pH during mechanosensing in *Arabidopsis* roots. Plant Cell. **21**, 2341–2356.

Mori, I.C., Iida, H., Tsuji, F.I., Isobe, M., Uozumi, N., and Muto, S. (1998). Salicylic acid induces a cytosolic Ca^{2+} elevation in yeast. Biosci. Biotechnol. Biochem. **62**, 986–989.

Munemasa, S., Hossain, M.A., Nakamura, Y., Mori, I.C., and Murata, Y. (2011). The *Arabidopsis* calcium-dependent protein kinase, CPK6, functions as a positive regulator of methyl jasmonate signaling in guard cells. Plant Physiol. **155**, 553–561.

Navazio, L., Bewell, M.A., Siddiqua, A., Dickinson, G.D., Galione, A., and Sanders, D. (2000). Calcium release from the endoplasmic reticulum of higher plants elicited by the NADP metabolite nicotinic acid adenine dinucleotide phosphate. Proc. Natl Acad. Sci. U S A. **97**, 8693–8698.

Pan, Z., Zhao, Y., Zheng, Y., Liu, J., Jiang, X., and Guo, Y. (2012). A high-throughput method for screening *Arabidopsis* mutants with disordered abiotic stress-induced calcium signal. Journal of Genetics and Genomics. **39**, 225–235.

Peiter, E., Maathuis, F.J., Mills, L.N., Knight, H., Pelloux, J., Hetherington, A.M., and Sanders, D. (2005). The vacuolar Ca^{2+}-activated channel TPC1 regulates germination and stomatal movement. Nature. **434**, 404–408.

Plieth, C. (2001). Plant calcium signaling and monitoring: pros and cons and recent experimental approaches. Protoplasma. **218**, 1–23.

Plieth, C. (2010). Signal percolation through plants and the shape of the calcium signature. Plant Signal Behav. **5**, 379–385.

Qi, Z., Stephens, N.R., and Spalding, E.P. (2006). Calcium entry mediated by GLR3.3, an *Arabidopsis* glutamate receptor with a broad agonist profile. Plant Physiol. **142**, 963–971.

Ranf, S., Grimmer, J., Pöschl, Y., Pecher, P., Chinchilla, D., Scheel, D., and Lee, J. (2012). Defense-related calcium signaling mutants uncovered via a quantitative high-throughput screen in *Arabidopsis thaliana*. Mol. Plant. **5**, 115–130.

Shigaki, T., and Hirschi, K.D. (2006). Diverse functions and molecular properties emerging for CAX cation/H+ exchangers in plants. Plant Biol. (Stuttg.). **8**, 419–429.

Souslova, E., Belousov, V., Lock, J., Stromblad, S., Kasparov, S., Bolshakov, A., Pinelis, V., Labas, Y., Lukyanov, S., Mayr, L., et al. (2007). Single fluorescent protein-based Ca^{2+} sensors with increased dynamic range. BMC Biotechnol. **7**, 37.

Sze, H., Liang, F., Hwang, I., Curran, A.C., and Harper, J.F. (2000). Diversity and regulation of plant Ca^{2+} pumps: insights from expression in yeast. Annu. Rev. Plant Physiol. Plant Mol. Biol. **51**, 433–462.

Tracy, F.E., Gilliham, M., Dodd, A.N., Webb, A.A., and Tester, M. (2008). NaCl-induced changes in cytosolic free Ca^{2+} in *Arabidopsis thaliana* are heterogeneous and modified by external ionic composition. Plant Cell Environ. **31**, 1063–1073.

Trewavas, A.J., and Malho, R. (1998). Ca^{2+} signalling in plant cells: the big network! Curr. Opin. Plant Biol. **1**, 428–433.

Vatsa, P., Chiltz, A., Bourque, S., Wendehenne, D., Garcia-Brugger, A., and Pugin, A. (2011). Involvement of putative glutamate receptors in plant defence signaling and NO production. Biochimie. **93**, 2095–2101.

Webb, A.A.R., McAinsh, M.R., Taylor, J.E., and Hetherington, A.M. (1996). Calcium ions as intracellular second messengers in higher plants. In Advances in Botanical Research, Callow, J.A., ed. (London: Academic Press), pp. 45–96.

Zhu, X., Caplan, J., Mamillapalli, P., Czymmek, K., and Dinesh-Kumar, S.P. (2010). Function of endoplasmic reticulum calcium ATPase in innate immunity-mediated programmed cell death. EMBO J. **29**, 1007–1018.